

Article

Low-Temperature Electrocatalytic Conversion of CO₂ to Liquid Fuels: Effect of the Cu Particle Size

Antonio de Lucas-Consuegra ^{1,*} , Juan Carlos Serrano-Ruiz ², Nuria Gutiérrez-Guerra ¹ and José Luis Valverde ¹

¹ Department of Chemical Engineering, School of Chemical Sciences and Technologies, University of Castilla-La Mancha, Avda. Camilo José Cela 12, 13005 Ciudad Real, Spain; nuriagutierrezguerra@gmail.com (N.G.-G.); joseluis.valverde@uclm.es (J.L.V.)

² Department of Engineering, Universidad Loyola Andalucía, Energía Solar, 1. Edifs. E, F and G, 41014 Seville, Spain; jcserrano@uloyola.es

* Correspondence: antonio.lconsuegra@uclm.es; Tel.: +34-926-295-300

Received: 30 July 2018; Accepted: 14 August 2018; Published: 20 August 2018



Abstract: A novel gas-phase electrocatalytic system based on a low-temperature proton exchange membrane (Sterion) was developed for the gas-phase electrocatalytic conversion of CO₂ to liquid fuels. This system achieved gas-phase electrocatalytic reduction of CO₂ at low temperatures (below 90 °C) over a Cu cathode by using water electrolysis-derived protons generated in-situ on an IrO₂ anode. Three Cu-based cathodes with varying metal particle sizes were prepared by supporting this metal on an activated carbon at three loadings (50, 20, and 10 wt %; 50% Cu-AC, 20% Cu-AC, and 10% Cu-AC, respectively). The cathodes were characterized by N₂ adsorption–desorption, temperature-programmed reduction (TPR), and X-ray diffraction (XRD) and their performance towards the electrocatalytic conversion of CO₂ was subsequently studied. The membrane electrode assembly (MEA) containing the cathode with the largest Cu particle size (50% Cu-AC, 40 nm) showed the highest CO₂ electrocatalytic activity per mole of Cu, with methyl formate being the main product. This higher electrocatalytic activity was attributed to the lower Cu–CO bonding strength over large Cu particles. Different product distributions were obtained over 20% Cu-AC and 10% Cu-AC, with acetaldehyde and methanol being the main reaction products, respectively. The CO₂ consumption rate increased with the applied current and reaction temperature.

Keywords: CO₂ electroreduction; CO₂ valorization; Cu catalyst; particle size; PEM; acetaldehyde production; methanol production

1. Introduction

Fossil fuels and biomass are the most common feedstocks for the production of liquid fuels. Since the burning of these feedstocks results in CO₂ emissions into the atmosphere, it is necessary to develop strategies for the upgrading of this gas into useful products. One of these approaches involves the recycling of CO₂ into sustainable hydrocarbon fuels [1] by different methods such as catalytic processes (e.g., hydrogenation to alkanes, alkenes or other oxygenated, or reforming with hydrocarbons) [2], biological processes [3], microwave and plasma systems [4–6], and photocatalytic and electrocatalytic routes [7]. Among these methods, the electrochemical reduction of CO₂ is highly interesting since it allows to directly transform CO₂ to syngas and light hydrocarbons with electricity, which may be obtained from renewable energy sources [1,8,9]. This approach is advantageous in that electrochemical cell reactors are typically compact, modular, and easy to scale-up. While electrolysis of CO₂ and/or H₂O can be carried out in solid oxide cells (SOCs) [10], the high temperatures required for these systems to operate (above 600 °C) usually result in catalyst sintering and stability losses.

In addition, high-temperature CO₂-H₂O co-electrolysis produces syngas as the only product, and further conversion steps (e.g., Fischer-Tropsch synthesis) are required to produce hydrocarbon fuels. Alternatively, low-temperature electrolyzers containing protonic exchange membranes (PEM) have been proposed to directly transform CO₂ into hydrocarbons and oxygenates [11–13]. Despite the overall single-pass conversions being typically low in these reactors, the unreacted CO₂ can be easily separated from the liquid fuels and recycled again to the reactor. The mild working conditions of these systems (typically below 90 °C and atmospheric pressure) facilitate the utilization of renewable energies such as solar heating and electrical energy for driving the electrochemical process. Moreover, unlike conventional catalytic hydrogenation of CO₂, PEM-based electrolyzers do not require external hydrogen since CO₂ directly reacts with the protons produced in-situ by water electrolysis [7]. These advantages have motivated researchers to investigate on gas-phase low-temperature CO₂ electroreduction [9,13–16], opening the way for incorporating renewable energies into the value chain of chemical industries. Professor Centi has developed most of these works with Pt, Fe, and Cu catalyst supported on a variety of carbonaceous materials such as carbon black, carbon nanofibers, and graphene, among others.

In this work, we carried out the electroreduction of CO₂ in the gas phase at low temperature over Cu cathodes. We performed a systematic study with three different Cu-based cathodic catalysts supported on a high-surface-area activated carbon. The main objective of the work was to study the influence of the Cu particle size on the electrocatalytic activity of the system. With this aim, three different membrane electrode assemblies (MEAs) were fabricated with three Cu cathodic catalysts having different metal loadings and particle sizes. These MEAs were characterized and subsequently used for the electrocatalytic conversion of CO₂ into synthetic fuels.

2. Results and Discussion

2.1. Characterization of The Cu Powder Catalysts and The Cu Electrodes

The different Cu powders and Cu cathodic-catalysts were characterized by N₂ adsorption–desorption, atomic absorption spectroscopy (AAS), temperature-programmed reduction (TPR), and X-ray diffraction (XRD). Table 1 shows the physicochemical properties of the activated carbon support (AC) and the three Cu cathodic-catalysts.

Table 1. Physicochemical properties of the support material, the catalysts, and the fresh electrodes.

Sample	Powder Metal Loading/wt %	Electrode Metal Weight/mg·cm ⁻²	Surface Area/m ² ·g ⁻¹	Total Pore Volume/cm ³ ·g ⁻¹	TPR-T _{max} /°C	Mean Particle Size from XRD/nm
AC	-	-	866	0.293	-	-
50% Cu-AC	55	0.22	773	0.186	171	40
20% Cu-AC	19	0.18	797	0.260	185	14
10% Cu-AC	12	0.16	817	0.274	193	12

The main difference between the three Cu cathodic catalysts is the metal loading. Thus, atomic absorption spectroscopy revealed metal loadings of 55, 19, and 12 wt % corresponding to electrode metal weights of 0.22, 0.18, and 0.16 mg·cm⁻² for the 50% Cu-AC, 20% Cu-AC, and 10% Cu-AC cathodic-catalysts, respectively. The electrocatalytic rates discussed below were normalized to the corresponding metal weight of the electrode.

The surface area and total pore volume of the different Cu cathodic-catalysts were determined by N₂ adsorption–desorption (Table 1). The activated carbon support showed high Langmuir areas and total pore volumes (866 m²·g⁻¹ and 0.293 cm³·g⁻¹, respectively), as previously reported in the literature [17,18]. As shown in Table 1, metal addition resulted in an important decrease of both the surface area and the total pore volume. As expected, the surface area and the total pore volume decreased with the metal loading, probably as a result of partial pore blockage by the metal

particles [18,19]. Combined IUPAC (International Union of Pure and Applied Chemistry) types I and IV N_2 adsorption–desorption isotherms (not shown) were obtained in all cases, revealing the presence of a microporous structure.

The TPR profiles of 50% Cu-AC, 20% Cu-AC, and 10% Cu-AC and the activated carbon support are shown in Figure 1. These TPR profiles result from the following sequential Cu reduction $Cu^{2+} \rightarrow Cu^+ \rightarrow Cu^0$ [20]. The first two reduction peaks at 171–193 °C and 223–276 °C (depending on the catalyst) can be attributed to the reduction of the more dispersed Cu particles and the reduction of CuO (II), respectively. The third reduction peak that appeared at 316–380 °C can be assigned to the reduction of Cu_2O (I). Finally, the peaks at higher temperatures are typically associated with the gasification of activated carbon and the reduction of surface oxygenated groups on the activated carbon support [21,22]. The temperature of the most intense consumption peak (T_{max}) is given in Table 1. The TPR profiles revealed that the interaction between the metal phase and the support varied depending on the metal particle size. Thus, stronger interactions were obtained for those catalysts having smaller Cu particles since T_{max} decreased with the Cu particle size (Table 1) [20,23,24]. Thus, the reducibility of the catalysts followed the sequence: 50% Cu-AC > 20% Cu-AC > 10% Cu-AC. Furthermore, given the TPR profiles, 400 °C was selected as a suitable reduction temperature for ensuring complete metal activation while maintaining the surface properties of the support.

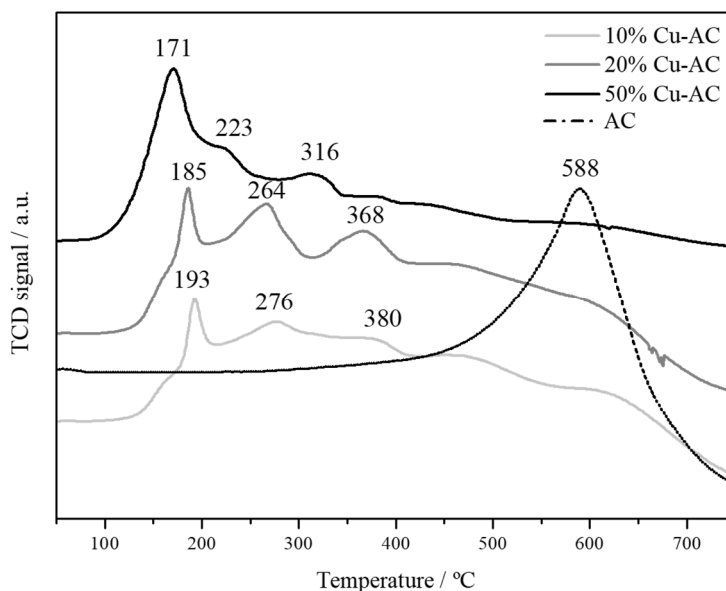


Figure 1. Temperature-programmed reduction (TPR) profiles of the fresh catalysts and the activated carbon support.

Figure 2 shows the XRD patterns of the powder catalyst 50% Cu-AC before and after the reduction treatment at 400 °C. No significant differences were appreciated between the three Cu-AC powder catalysts. As shown in Figure 2a, diffraction peaks corresponding to metallic copper (Cu) and copper oxide (Cu_2O and CuO) were observed before the reduction treatment. The main diffraction Cu peaks were (111), (200), (220), and (331) observed at 43.3, 50.4, 74.1, and 89.8°, respectively. These peaks are associated with a metallic Cu phase with face-centered cubic (FCC) crystalline structure (JCPDS, 85–1326). Diffraction peaks corresponding to Cu_2O (JCPDS, 78–2076) and CuO (JCPDS, 80–1917) were also observed, in line with the TPR results (Figure 1). However, these peaks were lower in intensity as compared to those of metallic copper. Figure 2b shows the XRD patterns of the catalysts after the reduction treatment. As shown by the XRD patterns, only peaks corresponding to metallic Cu were observed at $2\theta = 43.3, 50.4, 74.1,$ and 90° for the (111), (200), (220), and (331) planes. These results revealed that Cu was completely reduced at 400 °C, as anticipated by the TPR profiles. Additionally,

the metal precursor was completely calcined, since no peaks corresponding to the metal precursor were observed in the XRD patterns. The mean Cu particle sizes of the different catalysts were estimated using the Scherrer equation, and the results are summarized in Table 1. As expected, the mean Cu particle size increased significantly with the metal loading. The Cu particle sizes obtained herein (10–40 nm) were similar to those measured for similar electrocatalytic systems prepared by direct impregnation with Cu precursor solutions [16,17,25].

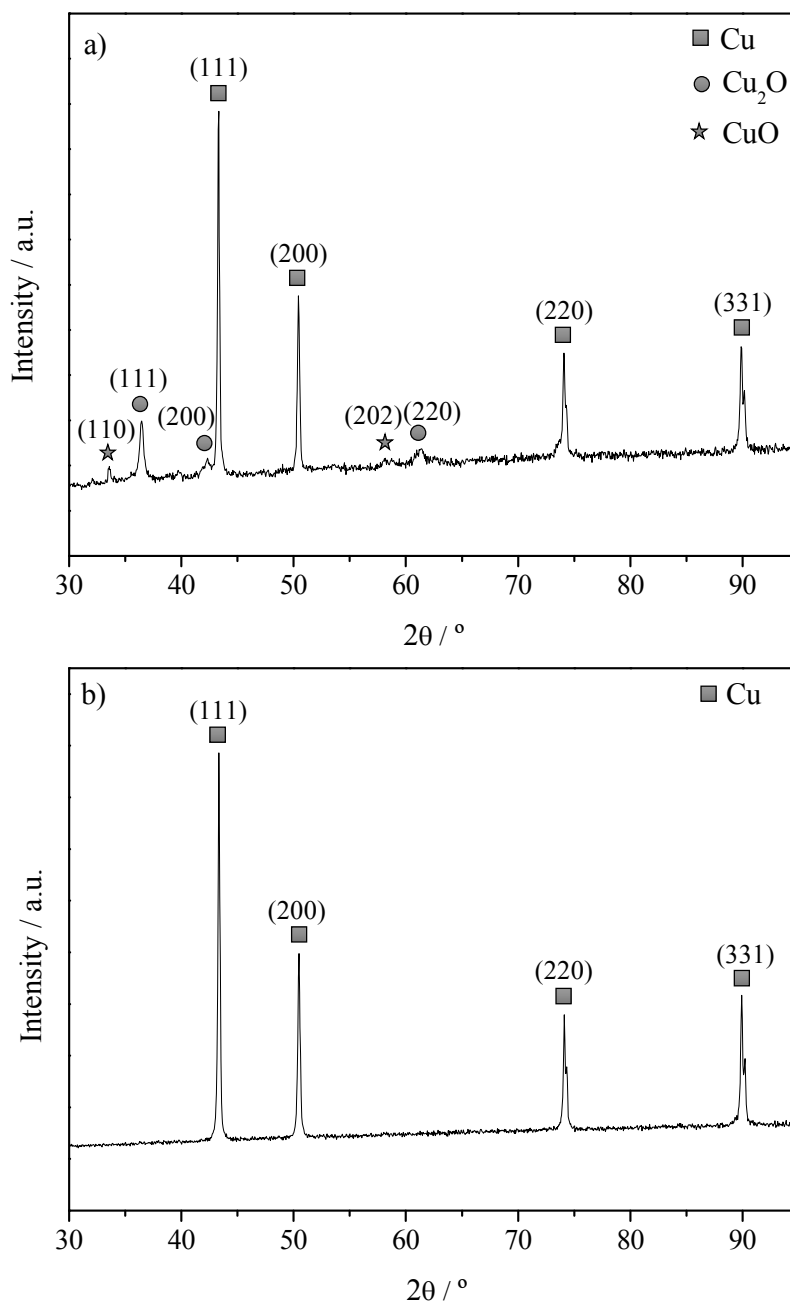
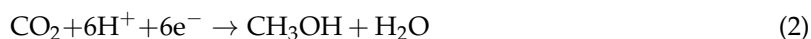
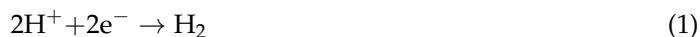


Figure 2. X-ray diffraction (XRD) patterns of 50% Cu-AC supported on carbon paper substrates: (a) before reduction at 400 °C and (b) after reduction at 400 °C.

2.2. CO_2 Conversion Electrocatalytic Experiments

Figure 3 shows the production rates of different compounds as a function of the time on stream during the electroreduction of CO_2 at a constant applied current of -20 mA and 90 °C. Note that no products were obtained under open circuit conditions (OCC, no current application). A constant

current of -20 mA was subsequently applied at 90 °C for approximately 350 min under the same reaction atmosphere. This polarization was maintained until products were obtained at a steady state rate. During this current application step, hydrogen (not shown in Figure 3, reaction (1)) and different products such as methanol, acetaldehyde, methyl formate, acetone, and n-propanol were obtained by reactions (2)–(6), respectively:



Most of these products have been previously obtained during the electrocatalytic conversion of CO_2 on Fe, Co, Pt, and Cu supported on carbon nanotubes [15,16,26–28] and Cu supported on different carbonaceous supports (activated carbon, carbon nanofibers, and graphite) [17] at similar temperatures. These products reached maximum production rates after ca. 300 min on stream and decreased upon OCC. A slow dynamic behavior was observed (the steady state was reached after 4–5 h of reaction), and this can be attributed to the high residence times used herein. At this point it should be mentioned that low Faradaic efficiencies to hydrocarbon products (below 10%) were obtained in all the experiments. This is due to the high kinetics of the hydrogen evolution reaction (reaction (1)) vs. hydrocarbon formation reactions (reactions (2)–(6)) due to the low surface concentration of CO_2 .

The configuration used herein is advantageous in that it allows the direct supply of H^+ (more reactive than H_2) to the cathodic side of the cell. This configuration allows lower temperatures (around 90 °C) as compared to catalytic CO_2 hydrogenation processes (above 250 °C) [21,29–31].

Finally, in all experiments, the cathodic side of the cell was purged with N_2 (30 $\text{NmL}\cdot\text{min}^{-1}$) and returned to OCC to remove all the products for subsequent reaction experiments. Sample 50% Cu-AC showed the highest intrinsic electrocatalytic activity among the three cathodic-catalyst studied herein. This higher electrocatalytic activity can be associated with the higher Cu particle size of 50% Cu-AC. Thus, large Cu particles have been previously reported to favor the formation of reaction products by reducing the strength of the metal–CO interaction [32]. In the electroreduction of CO_2 , CO_2 is adsorbed on active centers and subsequently converted into CO and O_2 . Since this adsorbed CO is more reactive than CO_2 , it reacts with protons to generate the different products observed. This reaction is favored on large Cu particles. Since small Cu particles adsorb CO more strongly than large particles, the subsequent reaction of CO is hindered on small Cu particles, leading to CO and H_2 as the main products [32].

With regard to the composition of the reaction products, methyl formate was the main reaction product over 50% Cu-AC, followed by acetaldehyde and methanol. Acetaldehyde and methanol were the main reaction products obtained over samples 20% Cu-AC and 10% Cu-AC, respectively. In line with our results, acetaldehyde and methanol were previously obtained as main products over Cu-AC catalysts [17]. In the case of catalyst 50% Cu-AC, the high Cu particle size favored the production of methyl formate by dehydrogenation of methanol Reaction (7), as previously reported [33].



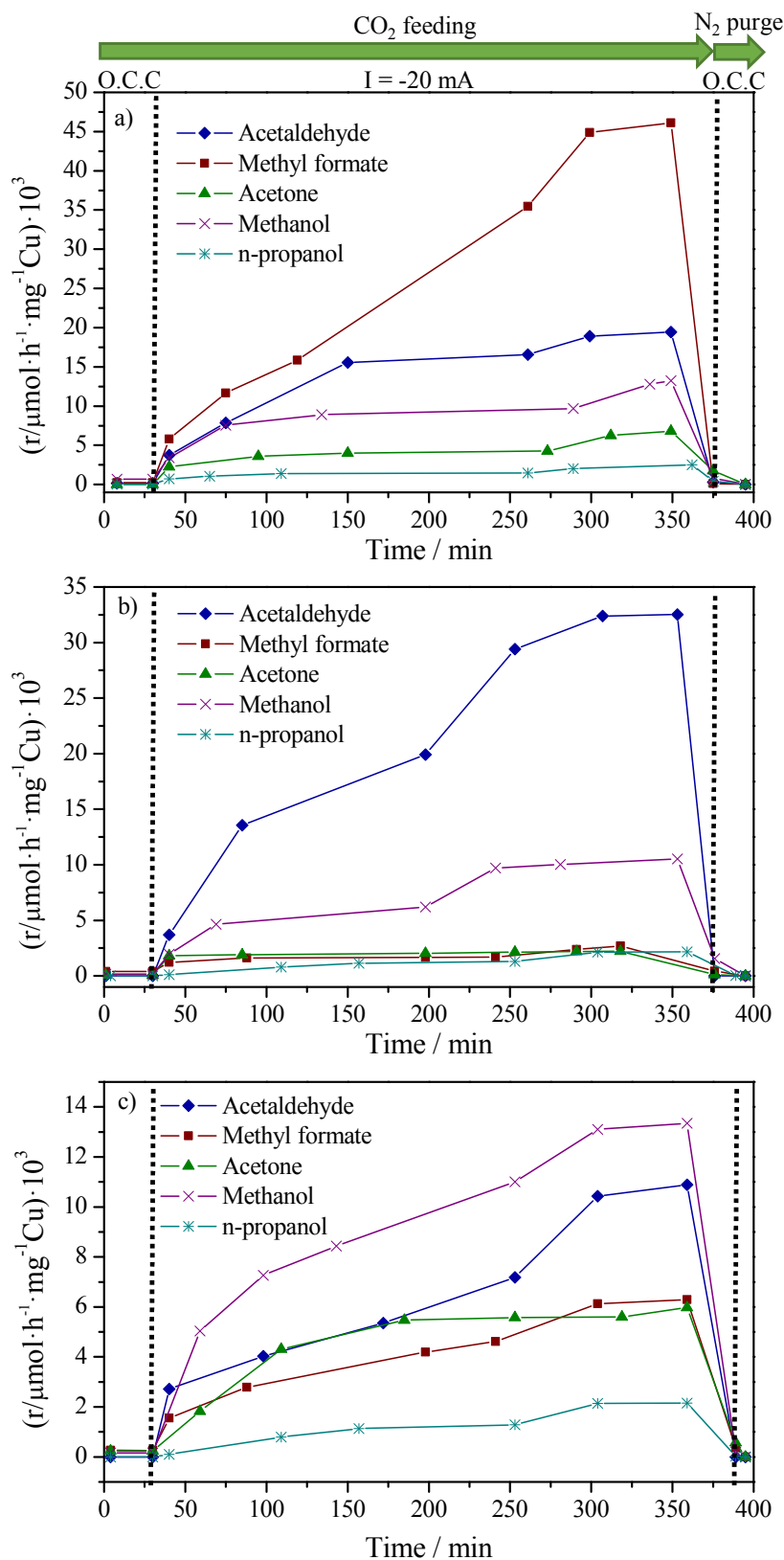


Figure 3. Time-on-stream variation of the rate of production for the different products at a constant current of -20 mA over the cathodic-catalysts on carbon paper substrates: (a) 50% Cu-AC, (b) 20% Cu-AC, and (c) 10% Cu-AC. Conditions: temperature = 90 °C, $F_{(\text{CO}_2)}$, cathode = 1.65 $\text{NmL}\cdot\text{min}^{-1}$ and $F_{(\text{H}_2\text{O})}$, anode = 6 $\text{NmL}\cdot\text{min}^{-1}$.

Figure 4a,b summarize the effect of the applied current and the reaction temperature on the steady state CO_2 consumption rate (after 350 min of polarization), respectively. The reaction rates were normalized by the amount of Cu deposited on each cathodic-catalyst. In line with the previous experiments, sample 50% Cu-AC showed larger electrocatalytic activities than samples 20% Cu-AC and 10% Cu-AC for all the reaction conditions studied. As expected, the consumption rate of CO_2 increased with the applied current, most likely because of an increase in the electrochemical supply of H^+ . In line with previous studies [15], an increase in the reaction temperature also resulted in higher electrocatalytic activities for all the catalysts tested. While the kinetics of the electrochemical reactions can be improved by increasing the temperature [34], the protonic membrane prevented us from testing the system above $90\text{ }^\circ\text{C}$ since its stability and conductivity under appropriate humidity conditions is not ensured at these conditions.

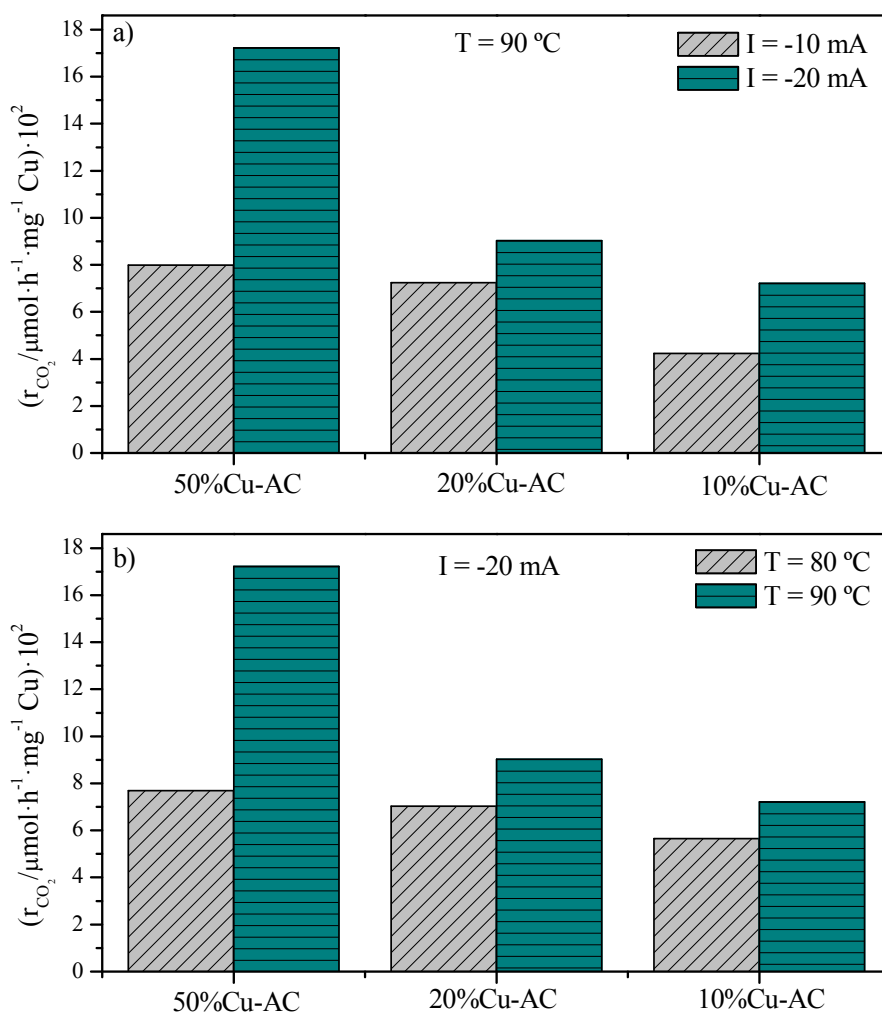


Figure 4. (a) Effect of the current at $90\text{ }^\circ\text{C}$ and (b) temperature at $I = -20\text{ mA}$ on the steady state CO_2 consumption rate for the cathodic-catalysts 50% Cu-AC, 20% Cu-AC, and 10% Cu-AC. Conditions: $F_{(\text{CO}_2)}$, cathode = $1.65\text{ NmL}\cdot\text{min}^{-1}$ y $F_{(\text{H}_2\text{O})}$, anode = $6\text{ NmL}\cdot\text{min}^{-1}$.

Finally, we calculated the energy consumption for the three different cathodic-catalysts evaluated. The three different MEAs were compared at $90\text{ }^\circ\text{C}$ and -20 mA . The overall energy consumption for CO_2 conversion ($\text{kW}\cdot\text{h}\cdot\text{mol}^{-1}\text{ CO}_2$) and the energy consumption for the production of methanol ($\text{kW}\cdot\text{h}\cdot\text{mol}^{-1}\text{ CH}_3\text{OH}$), acetaldehyde ($\text{kW}\cdot\text{h}\cdot\text{mol}^{-1}\text{ CH}_3\text{CHO}$), and methyl formate ($\text{kW}\cdot\text{h}\cdot\text{mol}^{-1}\text{ HCO}_2\text{CH}_3$) were calculated. As indicated above, the cathodic-catalyst with the highest metal loading, 50% Cu-AC, showed the highest electrocatalytic activity. This catalyst showed the lowest energy

consumption for the conversion of CO₂ (119.01 kW·h·mol⁻¹) among the catalysts tested. In addition, the MEA containing 50% Cu-AC consumed less energy per kg of methanol, acetaldehyde, and methyl formate (1549, 1054, and 444 kW·h·mol⁻¹, respectively) than the other two.

3. Materials and Methods

Cu catalysts supported on activated carbon were used as cathodes for the electrochemical reduction of CO₂, while Ir (IV) oxide (IrO₂) supported on carbon was used as a cell anode.

A commercial high surface area activated carbon (Sigma Aldrich, St. Louis, MO, USA) was used as a support. Metal particles were impregnated on activated carbon under vacuum at room conditions using an ethanolic precursor solution of Cu(NO₃)₃·3H₂O (Panreac, Barcelona, Spain) in a rotary evaporator. The catalysts were dried at 120 °C overnight and then calcined for 2 h at 350 °C in an N₂ atmosphere. A final reduction step under H₂ at 400 °C for 2 h was performed with a heating rate of 5 °C·min⁻¹. Three different catalysts were prepared with total Cu loadings of 50, 20, and 10 wt % (50% Cu-AC, 20% Cu-AC, and 10% Cu-AC, respectively).

The catalyst inks were prepared by mixing appropriate amounts of the different catalysts; IrO₂ commercial catalyst powders (Alfa Aesar, Haverhill, MA, USA, 99% for the anode, and Cu-activated-carbon powder for the cathode) with a Nafion solution (5 wt %, Aldrich Chemistry, St. Louis, MO, USA, Nafion[®] 117 solution) in isopropanol (Sigma Aldrich) containing a Nafion/solvent volume ratio of 0.04. IrO₂ was selected as an anode as in conventional PEM water electrolyzers [17]. The different inks were deposited on carbon paper (Fuel Cell Earth, Woburn, MA, USA) substrates with a geometric surface area for both electrodes of 12.56 cm² (circular electrode) at 65 °C. A commercial proton conducting Sterion[®] membrane (Hydrogen Works) was used as the electrolyte. Prior to use, the Sterion[®] membrane was successively pre-treated at 100 °C for 2 h in H₂O₂ and then into H₂SO₄ (to promote activation), and finally in deionized water to wash it. Then, the membrane electrode assembly (MEA) was prepared by sandwiching the membrane between the electrodes. Finally, the whole system was hot-pressed under heating conditions at 120 °C, and a final pressure of 1 metric ton was applied for 3 min.

The Cu metal loading on the powder catalysts was measured by Atomic Absorption Spectroscopy (AAS) using a SPECTRA 220FS analyzer. The sample (ca. 0.5 g) was dissolved in a mixture containing 2 mL of HCl, 3 mL of HF, and 2 mL of H₂O₂ followed by microwave digestion at 250 °C. The surface area and volume porosity of the different materials were measured using a Micromeritics ASAP 2010. N₂ was used as the sorbate at -193 °C, and the microporosity was measured by the Howath-Kawazoe (HK) method. Prior to the analyses, the samples were outgassed at 180 °C under vacuum (5 × 10⁻³ Torr) for 12 h. Temperature Programmed Reduction (TPR) experiments were conducted on a commercial Micromeritics AutoChem 2950 HP unit provided with a thermal conductivity (TCD) detector. The samples (ca. 0.15 g) were loaded into a U-shaped reactor and ramped from room temperature up to 900 °C (10 °C·min⁻¹) under a reducing H₂/Ar gas mixture of 17.5% v/v (60 cm³·min⁻¹). X-Ray diffraction analysis (XRD) were conducted on the Cu-AC powder catalysts prior and after reduction with a Philips PW-1710 instrument, using Ni-filtered Cu K α radiation ($\lambda = 1.5404 \text{ \AA}$). The samples were analyzed at a rate of 0.02°·step⁻¹ over a 2 θ range of 20–80° (scan time 2 s·step⁻¹) and the obtained spectra were compared with the corresponding JCPDS-ICDD references.

CO₂ electro-reduction experiments were performed in an electrochemical cell reactor working at room pressure conditions [17]. Water was introduced into the anode side using a saturator. The water content in the anodic feed stream (25% H₂O/N₂) was controlled by the heating the saturator at 65 °C. All the pipelines downstream from the saturator were heated to avoid condensation. On the anode side, water electro-oxidation was carried out on IrO₂ to generate protons across the Sterion[®] membrane. The water stream was also used to hydrate the Sterion[®] membrane and to keep its ionic conductivity under working conditions [16]. The cathodic side of the cell operates under a gas flow of pure CO₂ (Praxair Inc. certified standards 99.999% purity, Danbury, CT, USA). Both gas flow rates (N₂ for the anode and CO₂ for the cathode) were controlled by mass flowmeters (Brooks, Seattle, WA, USA).

The electrocatalytic experiments were carried out at atmospheric pressure with an overall gas flow rate of $0.5 \text{ NmL}\cdot\text{min}^{-1}$ of CO_2 for the cathodic stream and $6 \text{ NmL}\cdot\text{min}^{-1}$ for the anodic stream working at 80 and 90 °C. The reactant and products outlet stream from the cathodic chamber were analyzed by using a double channel gas chromatograph (Bruker 450-GC) equipped with Haysep Q-Molsieve 13X consecutive columns and flame ionization detectors (FIDs). Hydrogen, methanol, acetaldehyde, methyl formate, acetone, and n-propanol were the reaction products detected. The carbon atom balance closed within a 10% error. A potentiostat/galvanostat (Voltalab 21, Radiometer Analytical, Lyon, France) was used for the different applied polarizations, and the two electrodes were connected to the potentiostat by using gold wires.

4. Conclusions

Three different Cu-based cathodic-catalysts with Cu loadings of 50, 20, and 10 wt % were synthesized by impregnation, characterized, and tested in the electrocatalytic conversion of CO_2 .

50% Cu-AC showed the highest CO_2 electrocatalytic activity among the catalysts tested under all the explored reaction conditions. These results could be explained by the higher Cu particle size of this material. Considering that CO is an important intermediate in the process, large Cu particles are believed to favor electroreduction by weakening the metal–CO interaction.

Methyl formate was the main reaction product for 50% Cu-AC, while acetaldehyde and methanol were the main products for 20% Cu-AC and 10% Cu-AC, respectively. This fact can be attributed to the higher particle size of Cu that favored the production of methyl formate via dehydrogenation of methanol.

The CO_2 consumption rate increased with the applied current and the reaction temperature due to an enhancement of the kinetic of the electrocatalytic reactions.

Finally, 50% Cu-AC showed the highest electrocatalytic activity and the lowest energy consumption values for the conversion of CO_2 ($119 \text{ kW}\cdot\text{h}\cdot\text{mol}^{-1}$). In addition, the MEA containing 50% of Cu consumed less energy per kg of methanol, acetaldehyde, and methyl formate than the other two MEAs containing less amount of Cu.

Author Contributions: J.L.V. conceived the project, N.G.-G. performed the experiments and J.C.S.-R. and A.d.L.-C. wrote the manuscript.

Funding: Financial Support received from the Spanish “Ministerio de Ciencia e Innovación” (Project CTQ2016-75491-R) and from Abengoa Research is gratefully acknowledged. JCSR would like to acknowledge the Spanish Ministry of Science, Innovation and Universities for financial support under the Ramón y Cajal Program (grant RYC-2015-19230).

Conflicts of Interest: The authors declare no conflict of interest. The founding sponsors had no role in the design of the study; in the collection, analyses, or interpretation of data; in the writing of the manuscript, and in the decision to publish the results.

References

1. Umeyama, T.; Imahori, H. Carbon nanotube-modified electrodes for solar energy conversion. *Energy Environ. Sci.* **2008**, *1*, 120–133. [[CrossRef](#)]
2. Bansode, A.; Urakawa, A. Towards full one-pass conversion of carbon dioxide to methanol and methanol-derived products. *J. Catal.* **2014**, *309*, 66–70. [[CrossRef](#)]
3. Sekar, N.; Ramasamy, R.P. Recent advances in photosynthetic energy conversion. *J. Photochem. Photobiol. C-Photochem. Rev.* **2015**, *22*, 19–33. [[CrossRef](#)]
4. Khiabani, N.H.; Yaghmaee, M.S.; Sarani, A.; Shokri, B. Synthesis-gas production from CH_4 - CO_2 -Ar via microwave plasma torch. *Adv. Stud. Theor. Phys.* **2012**, *6*, 1273–1287.
5. Yu, Q.; Kong, M.; Liu, T.; Fei, J.; Zheng, X. Characteristics of the decomposition of CO_2 in a dielectric packed-bed plasma reactor. *Plasma Chem. Plasma Process.* **2012**, *32*, 153–163. [[CrossRef](#)]
6. Rahemi, N.; Haghighi, M.; Babaluo, A.A.; Jafari, M.F.; Allahyari, S. CO_2 reforming of methane over Ni-Cu/ Al_2O_3 - ZrO_2 nanocatalyst: The influence of plasma treatment and process conditions on catalytic properties and performance. *Korean J. Chem. Eng.* **2014**, *31*, 1553–1563. [[CrossRef](#)]

7. Centi, G.; Perathoner, S. Opportunities and prospects in the chemical recycling of carbon dioxide to fuels. *Catal. Today* **2009**, *148*, 191–205. [[CrossRef](#)]
8. Albo, J.; Alvarez-Guerra, M.; Castaño, P.; Irabien, A. Towards the electrochemical conversion of carbon dioxide into methanol. *Green Chem.* **2015**, *17*, 2304–2324. [[CrossRef](#)]
9. Centi, G.; Quadrelli, E.A.; Perathoner, S. Catalysis for CO₂ conversion: A key technology for rapid introduction of renewable energy in the value chain of chemical industries. *Energy Environ. Sci.* **2013**, *6*, 1711–1731. [[CrossRef](#)]
10. Graves, C.; Ebbesen, S.D.; Mogensen, M. Co-electrolysis of CO₂ and H₂O in solid oxide cells: Performance and durability. *Solid State Ionics* **2011**, *192*, 398–403. [[CrossRef](#)]
11. Blomen, E.; Hendriks, C.; Neele, F. Capture technologies: improvements and promising developments. *Energy Procedia* **2009**, *1*, 1505–1512. [[CrossRef](#)]
12. Yamataka, I.; Tabata, K.; Mino, W.; Furusawa, T. Electroreduction of Carbon Dioxide to Carbon Monoxide by Co-pthalocyanine Electrocatalyst under Ambient Conditions. *ISIJ Int.* **2015**, *55*, 399–403. [[CrossRef](#)]
13. Ampelli, C.; Genovese, C.; Perathoner, S.; Centi, G.; Errahali, M.; Gatti, G.; Marchese, L. An electrochemical reactor for the CO₂ reduction in gas phase by using conductive polymer based electrocatalysts. *Chem. Eng. Trans.* **2014**, *41*, 13–18.
14. Lee, K.; Zhang, J.; Wang, H.; Wilkinson, D.P. Progress in the synthesis of carbon nanotube-and nanofiber-supported Pt electrocatalysts for PEM fuel cell catalysis. *J. Appl. Electrochem.* **2006**, *36*, 507–522. [[CrossRef](#)]
15. Genovese, C.; Ampelli, C.; Perathoner, S.; Centi, G. Electrocatalytic conversion of CO₂ to liquid fuels using nanocarbon-based electrodes. *J. Energy Chem.* **2013**, *22*, 202–213. [[CrossRef](#)]
16. Genovese, C.; Ampelli, C.; Perathoner, S.; Centi, G. Electrocatalytic conversion of CO₂ on carbon nanotube-based electrodes for producing solar fuels. *J. Catal.* **2013**, *308*, 237–249. [[CrossRef](#)]
17. Gutiérrez-Guerra, N.; Moreno-López, L.; Serrano-Ruiz, J.C.; Valverde, J.L.; de Lucas-Consuegra, A. Gas phase electrocatalytic conversion of CO₂ to syn-fuels on Cu based catalysts-electrodes. *Appl. Catal. B-Environ.* **2016**, *188*, 272–282.
18. Rodríguez-Reinoso, F. The role of carbon materials in heterogeneous catalysis. *Carbon* **1998**, *36*, 159–175. [[CrossRef](#)]
19. Molina-Sabio, M.; Perez, V.; Rodríguez-Reinoso, F. Impregnation of activated carbon with chromium and copper salts: Effect of porosity and metal content. *Carbon* **1994**, *32*, 1259–1265. [[CrossRef](#)]
20. Zhang, G.; Li, Z.; Zheng, H.; Fu, T.; Ju, Y.; Wang, Y. Influence of the surface oxygenated groups of activated carbon on preparation of a nano Cu/AC catalyst and heterogeneous catalysis in the oxidative carbonylation of methanol. *Appl. Catal. B-Environ.* **2015**, *179*, 95–105. [[CrossRef](#)]
21. Díez-Ramírez, J.; Sánchez, P.; Rodríguez-Gómez, A.; Valverde, J.L.; Dorado, F. Carbon nanofiber-based palladium/zinc catalysts for the hydrogenation of carbon dioxide to methanol at atmospheric pressure. *Ind. Eng. Chem. Res.* **2016**, *55*, 3556–3567. [[CrossRef](#)]
22. Román-Martínez, M.C.; Cazorla-Amorós, D.; Linares-Solano, A.; De Lecea, C.S.M. TPD and TPR characterization of carbonaceous supports and Pt/C catalysts. *Carbon* **1993**, *31*, 895–902. [[CrossRef](#)]
23. Gil, S.; Muñoz, L.; Sánchez-Silva, L.; Romero, A.; Valverde, J.L. Synthesis and characterization of Au supported on carbonaceous material-based catalysts for the selective oxidation of glycerol. *Chem. Eng. J.* **2011**, *172*, 418–429. [[CrossRef](#)]
24. Trépanier, M.; Dalai, A.K.; Abatzoglou, N. Synthesis of CNT-supported cobalt nanoparticle catalysts using a microemulsion technique: Role of nanoparticle size on reducibility, activity and selectivity in Fischer-Tropsch reactions. *Appl. Catal. A-Gen.* **2010**, *374*, 79–86. [[CrossRef](#)]
25. Karelavic, A.; Ruiz, P. The role of copper particle size in low pressure methanol synthesis via CO₂ hydrogenation over Cu/ZnO catalysts. *Catal. Sci. Technol.* **2015**, *5*, 869–881. [[CrossRef](#)]
26. Genovese, C.; Ampelli, C.; Perathoner, S.; Centi, G. A gas-phase electrochemical reactor for carbon dioxide reduction back to liquid fuels. *Chem. Eng. Trans.* **2013**, *32*, 289–294.
27. Gangeri, M.; Perathoner, S.; Caudo, S.; Centi, G.; Amadou, J.; Begin, D.; Schlögl, R. Fe and Pt carbon nanotubes for the electrocatalytic conversion of carbon dioxide to oxygenates. *Catal. Today* **2009**, *143*, 57–63. [[CrossRef](#)]
28. Centi, G.; Perathoner, S.; Winè, G.; Gangeri, M. Electrocatalytic conversion of CO₂ to long carbon-chain hydrocarbons. *Green Chem.* **2007**, *9*, 671–678. [[CrossRef](#)]

29. Ahouari, H.; Soualah, A.; Le Valant, A.; Pinard, L.; Magnoux, P.; Pouilloux, Y. Methanol synthesis from CO₂ hydrogenation over copper based catalysts. *React. Kinet. Mech. Catal.* **2013**, *110*, 131–145. [[CrossRef](#)]
30. Díez-Ramírez, J.; Valverde, J.L.; Sánchez, P.; Dorado, F. CO₂ hydrogenation to methanol at atmospheric pressure: influence of the preparation method of Pd/ZnO catalysts. *Catal. Lett.* **2016**, *146*, 373–382. [[CrossRef](#)]
31. Díez-Ramírez, J.; Dorado, F.; de la Osa, A.R.; Valverde, J.L.; Sánchez, P. Hydrogenation of CO₂ to methanol at atmospheric pressure over Cu/ZnO catalysts: influence of the calcination, reduction, and metal loading. *Ind. Eng. Chem. Res.* **2017**, *56*, 1979–1987. [[CrossRef](#)]
32. Reske, R.; Mistry, H.; Behafarid, F.; Roldan Cuenya, B.; Strasser, P. Particle size effects in the catalytic electroreduction of CO₂ on Cu nanoparticles. *J. Am. Chem. Soc.* **2014**, *136*, 6978–6986. [[CrossRef](#)] [[PubMed](#)]
33. Tonner, S.P.; Trimm, D.L.; Wainwright, M.S.; Cant, N.W. Dehydrogenation of methanol to methyl formate over copper catalysts. *Ind. Eng. Chem. Prod. Res. Dev.* **1984**, *23*, 384–388. [[CrossRef](#)]
34. Caravaca, A.; Sapountzi, F.M.; de Lucas-Consuegra, A.; Molina-Mora, C.; Dorado, F.; Valverde, J.L. Electrochemical reforming of ethanol–water solutions for pure H₂ production in a PEM electrolysis cell. *Int. J. Hydrogen Energy* **2012**, *37*, 9504–9513. [[CrossRef](#)]



© 2018 by the authors. Licensee MDPI, Basel, Switzerland. This article is an open access article distributed under the terms and conditions of the Creative Commons Attribution (CC BY) license (<http://creativecommons.org/licenses/by/4.0/>).